Available online at www.sciencedirect.com
ScienceDirect
Polymer 48 (2007) 1930–1939
polymer
www.elsevier.com/locate/polymer

UV reactive polymers for refractive index modulation based on the photo-Fries rearrangement

T. Höfler [a], T. Grießer [a], X. Gstrein [b], G. Trimmel [a], G. Jakopic [c], W. Kern [a,*]

[a] *Institute for Chemistry and Technology of Organic Materials, Graz University of Technology, Stremayrgasse 16, A-8010 Graz, Austria*
[b] *Polymer Competence Center Leoben GmbH, A-8700 Leoben, Austria*
[c] *Institute for Nanostructured Materials and Photonics, Joanneum Research, A-8160 Weiz, Austria*

Received 12 September 2006; received in revised form 15 January 2007; accepted 20 January 2007
Available online 25 January 2007

Abstract

In this study we report on the synthesis and characterization of photoreactive polymers which display large changes in their refractive index upon UV irradiation. These polymers contain aromatic ester groups which undergo a photo-Fries rearrangement from aryl esters to hydroxyketones. The polymers under investigation were poly(4-acetoxystyrene) and two derivatives of polynorbornene, poly(bicyclo[2.2.1]hept-5-ene-2-carboxylic acid, phenyl ester) and poly(bicyclo[2.2.1]hept-5-ene-2,3-dicarboxylic acid, diphenyl ester). The kinetics of the photoreaction was studied by FTIR spectroscopy. Ellipsometric measurements of thin films showed that the photo-Fries rearrangement causes a large increase of the refractive indices in these polymers (between +0.03 and +0.05). The modulation of the refractive index is of interest for applications in the field of optics and data storage. The photoreaction also leads to an increase in surface energy as evidenced by contact angle measurements with water and diiodomethane as test liquids.

Keywords: Photo-Fries rearrangement; Refractive index; Photoreactive polymer

1. Introduction

Polymers with tunable refractive index are applied for optical data storage (e.g. by holography), optical elements such as distributed feedback (DFB) lasers as well as for inscribing of waveguide structures in planar films [1]. Over the past years numerous materials have been reported which provide the possibility to inscribe refractive index patterns by UV photolithography. Photopolymerizable acrylate resins, poly(vinyl cinnamate) which undergoes a [2 + 2] cyclodimerization, as well as polymers bearing azobenzene moieties (reversible *cis–trans* photoisomerization of the azobenzene chromophore) are among these recording materials [2]. However, only a few recording materials operate at deep UV wavelengths (<300 nm) and simultaneously offer the advantage of a well defined photochemistry. In our previous work we reported on photo-induced refractive index changes in polymers containing thiocyanate groups [3]. In polymers such as poly(4-vinylbenzyl thiocyanate) the photoisomerization of thiocyanates (−SCN) to isothiocyanates (−NCS) results in refractive index changes (Δn approx. +0.03). Post-exposure modification with gaseous amines gives a further change in the refractive index [4]. Only recently we have transferred this photochemistry to poly(norbornenes) prepared by ring-opening metathesis polymerization (ROMP) [5]. This polymerization process offers the advantage that well defined polymers and block copolymers can be obtained in a convenient fashion by living polymerization using ruthenium-based catalysts [6,7].

In search of alternative photoreactions which give a large increase in the refractive index of polymers we now investigated the so-called photo-Fries reaction. It is well known that aryl esters of carboxylic acids undergo photolytic reactions upon irradiation with ultraviolet light (200–250 nm).

* Corresponding author.
E-mail address: w.kern@tugraz.at (W. Kern).

0032-3861/$ - see front matter © 2007 Elsevier Ltd. All rights reserved.
doi:10.1016/j.polymer.2007.01.041

The photo-Fries rearrangement transforms aryl esters to hydroxyketones as first observed by Anderson and Reese in 1960 [8,9]. This photoreaction mainly yields a mixture of *ortho*- and *para*-hydroxyketones. Phenols and decarboxylation products are obtained in side reactions. Scheme 1 presents a survey of the photolysis products of aryl esters.

Considering the refractive indices of two low-molecular weight model compounds, acetic acid phenyl ester ($n_D = 1.5035$) and the corresponding photo-Fries rearrangement product 2-hydroxyacetophenone ($n_D = 1.5584$) [10], it can be expected that the photo-Fries reaction results in significant changes of the refractive index. Indeed, such index changes have been claimed in the patent literature for holographic compositions [11].

Since discovery, it has taken a long time to elucidate the mechanism of the photo-Fries rearrangement. The generally accepted mechanism [12,13] proceeds via free radical intermediates as depicted in Scheme 1. Taking 4-*tert*-butylphenyl acetate as an example, Lochbrunner et al. [14] have shown that, as a first step, a cleavage of the C–O band occurs. This photolysis proceeds from an excited singlet (S_1) state. The photogenerated radicals can recombine and then yield a derivative of cyclohexadienone as the ''cage product'' (*ortho* and *para* products). Tautomerism then gives the hydroxyketone, which is the rearranged acyl migration product. For aromatic esters lacking additional substituents at the aromatic ring (e.g. phenyl acetate), the ratio of the *ortho*- and *para*-substituted compounds can be controlled by the reaction temperature. The ''escape product'' of the geminate radical pair is mainly phenol which is explained by hydrogen abstraction from the solvent. It is known that in aromatic esters a parallel reaction of the photo-Fries reaction can occur: the photodecarboxylation (photoextrusion of CO_2) [15] which has been found by Finnegan and Knutson [16], cf. Scheme 1. The photodecarboxylation of R–(CO–O)–R′ to give R–R′ proceeds from the S_1 state and a concerted (i.e. non-radical) mechanism has been proposed. Weiss et al. support the idea that in ester compounds R–(CO_2)–R′ intramolecular steric effects (e.g. substituents placed on the aryl rings) and intermolecular interactions (i.e. templating medium effects as provided by a polymer matrix) enhance the yield of the decarboxylation product R–R′. Generally, photodecarboxylation is enhanced in constrained media and at lower temperatures [17].

Bellus and Hrdlovic [18] investigated the photo-Fries reaction thoroughly and demonstrated the application of the photo-Fries rearrangement for preparative synthetic chemistry. Considering polymeric phenyl esters, polymers such as poly(4-acetoxystyrene) and poly(4-formyloxystyrene) have been investigated as positive resist materials for photolithography [19]. These polymers become increasingly soluble in alkaline media upon deep UV irradiation which is due to the formation of phenolic OH groups.

The photo-Fries rearrangement is an irreversible photoreaction yielding a stable product (similar to the SCN–NCS photoisomerization). The synthetic preparation of aryl esters and their polymers is convenient and a wide range of products are easily accessible. In addition to this, ester groups are compatible with a large number of transition-metal catalysts which facilitate catalytic polymerizations of functional monomers. These are important advantages for technological applications.

We started our investigation with the model polymer poly(4-acetoxystyrene) and transferred the concept of the photo-Fries reaction to poly(norbornene esters). The present paper describes the photo-induced reactions in thin films of poly(4-acetoxystyrene) and functional derivatives of polynorbornene, poly(bicyclo[2.2.1]hept-5-ene-2-carboxylic acid, phenyl ester) and poly(*endo*,*exo*-bicyclo[2.2.1]hept-5-ene-2,3-dicarboxylic acid, diphenyl ester). Upon UV illumination the esters rearrange and the corresponding hydroxyketones are formed. These processes have been monitored by FTIR and UV/vis spectroscopy. Furthermore ellipsometric measurements showed that the photo-Fries reaction causes significant changes of the polymer's refractive index. This provides a convenient way for refractive index patterning as required for data storage and waveguiding.

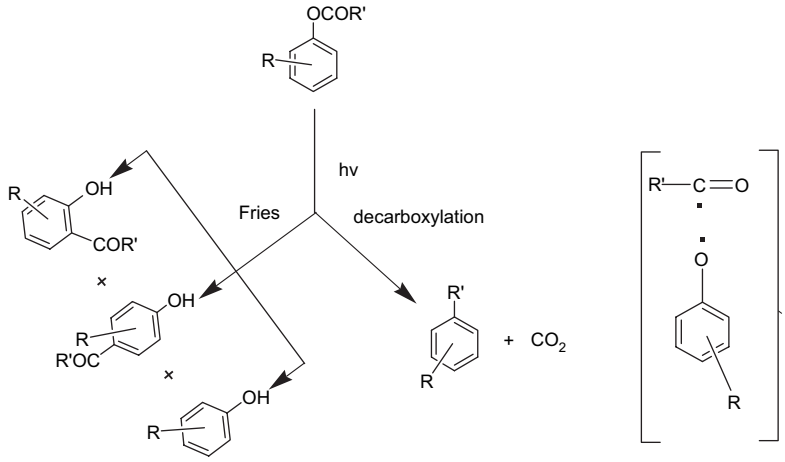

Scheme 1. General photoproducts of aryl esters by photo-Fries rearrangement (via a radical mechanism) and by decarboxylation (via a concerted mechanism). The radical pair which is generated upon UV irradiation is also represented in this scheme.

2. Experimental part

2.1. Materials

All materials were purchased from commercial sources. Fumaryl chloride was distilled for purification, toluene and dichloromethane were freshly distilled over appropriate drying agents (Na/K and CaH_2, respectively) under nitrogen atmosphere prior to use. All other chemicals were used without further purification.

2.2. Synthetic procedures

2.2.1. Synthesis of poly(4-acetoxystyrene) (poly-*1*)

For the synthesis of poly(4-acetoxystyrene) a literature procedure [19] was modified. Anhydrous toluene of 100 mL, 100 mg (0.61 mmol) of azo-bis-isobutyronitrile, and 10.6 g (65 mmol) of 4-acetoxystyrene (**1**) were placed in a round bottom flask and heated to 100 °C for 5 h under nitrogen atmosphere. The reaction mixture was precipitated with methanol and dried in vacuo. The yield of poly-**1** was 3.18 g (30%). $M_n = 13{,}800\ g\ mol^{-1}$; $M_w = 18{,}600\ g\ mol^{-1}$; PDI = 1.4 as determined by SEC. ^1H NMR (δ, 20 °C, $CDCl_3$, 500 MHz): 1.05–1.97 (m, 3H, CH_2–CH), 2.21 (s, 3H, CH_3), 6.25–7.11 (m, 4H, aromatic). FTIR (thin film on CaF_2, cm^{-1}): 3025 (w, aromatic ν_{CH}) 2983–2861 (m, aliphatic C–H) 1767 (s, C=O), 1694 (w), 1509 (m, aromatic C=C), 1423 (w), 1373 (m), 1215 (m, C–O–C ester), 1197 (m, C–O–C ester), 1020 (m), 911 (m), 846 (m, CH in *para*-substituted benzene). ^1H NMR and FTIR data are in good agreement with literature values [19].

2.2.2. Synthesis of bicyclo[2.2.1]hept-5-ene-2-carboxylic acid, phenyl ester (*2*) (mixture of the endo and exo forms)

Acryloyl chloride of 6.41 g (70.84 mmol) was dissolved in 60 mL of dry dichloromethane and cooled with an ice/water bath. Freshly distilled cyclopentadiene of 9.36 g (161.60 mmol) in 20 mL of dichloromethane was added dropwise to the solution, the cooling bath was removed, and the reaction mixture was stirred for 16 h at ambient temperature. The reaction mixture was cooled down again with ice/water bath, and 8.00 g (85.01 mmol) of phenol was added dropwise. The cooling bath was removed, and the reaction mixture was stirred for further 24 h at ambient temperature. Deionized H_2O of 200 mL was added, after phase separation the organic phase was extracted with diluted hydrochloric acid (1.5%), then with water and finally with aqueous Na_2CO_3 (10 wt.%) and subsequently dried over Na_2SO_4. The solvent was removed in vacuo. The residual crude product was purified by column chromatography (silica gel, cyclohexane/ethyl acetate (50:1)). Yield of compound **2**: 8.42 g (55%) of a yellowish oil.

^1H NMR (δ, 20 °C, $CDCl_3$, 500 MHz) only the signals of the *endo*-form are given (approx. 85% *endo*, 15% *exo*-form): 7.36 (m, 2H, $ph^{3,5}$), 7.20 (m, 1H, ph^4), 7.05 (m, 2H, $ph^{2,6}$), 6.27 (m, 1H, nb^5), 6.09 (m, 1H, nb^6), 3.39 (s, 1H, nb^1), 3.22 (m, 1H, nb^4), 2.98 (s, 1H, nb^2), 2.02 (m, 1H, nb^3), 1.57 (m, 2H, $nb^{3,7}$), 1.38 (d, 1H, nb^7). $^{13}C\{^1H\}$ NMR (δ, 20 °C, $CDCl_3$, 125 MHz): 173.4 (1C, –COO–), 151.0 (1C, ph^1), 138.3 (1C, nb^5), 132.3 (1C, nb^6), 129.3 (2C, $ph^{3,5}$), 125.7 (1C, ph^4), 121.7 (2C, $ph^{2,6}$), 49.9 (1C, nb^7), 46.1 (1C, nb^1), 43.8 (1C, nb^4), 42.8 (1C, nb^2), 29.5 (1C, nb^3). These data are in good agreement with the literature [20].

2.2.3. Poly(bicyclo[2.2.1]hept-5-ene-2-carboxylic acid, phenyl ester) (poly-*2*)

To a solution of 5.00 g (23.3 mmol) of monomer **2** in 45 mL of dry dichloromethane, 38.41 mg (0.046 mmol) of $[RuCl_2(PCy_3)(CHPh)]$ (Cy = cyclohexyl) dissolved in 10 mL of dry dichloromethane was added. The reaction mixture was stirred at room temperature for 24 h and then the reaction was stopped by adding 0.5 mL of ethylvinylether and the polymer was precipitated by slowly pouring the solution into an excess of cold methanol. The precipitate was dried in vacuo. Yield of poly-**2**: 4.056 g (81%) of a white solid. $M_n = 160{,}000\ g\ mol^{-1}$; $M_w = 307{,}000\ g\ mol^{-1}$; PDI = 1.9 (determined by SEC); T_g: 72.6 °C. ^1H NMR (δ, 20 °C, $CDCl_3$, 500 MHz): 7.25–7.00 (m, 5H, ph), 5.73 (m, 2H, CH=CH), 3.63–2.97 (m, 4H, nb), 2.56–2.16 (m, 2H, nb) 1.56 (d, 1H, nb). Elemental analysis: found C: 77.80%, H: 6.61%, O: 15.59%; calculated C: 78.48%, H: 6.59%, O: 14.93%. FTIR (thin film on CaF_2, cm^{-1}): 3057 (w, aromatic C–H), 3005–2856 (m, aliphatic C–H), 1745 (s, C=O), 1484 (m, aromatic C=C), 1454 (w), 1361 (w), 1193 (s, C–O–C ester), 1157 (s), 1130 (s).

2.2.4. (±)-endo,exo-Bicyclo[2.2.1]hept-5-ene-2,3-dicarboxylic acid, diphenyl ester (*3*)

Fumaryl chloride of 7.07 g (46.2 mmol) was dissolved in 60 mL of dry dichloromethane and cooled down with an ice/water bath. Freshly distilled cyclopentadiene of 6.11 g (92.4 mmol) in 20 mL dichloromethane was added dropwise to the solution, the cooling bath was removed, and the reaction mixture was stirred for 23 h at ambient temperature. The reaction mixture was cooled down again with an ice/water bath, and 10 g of phenol (161 mmol) and 11.0 g of pyridine (138.5 mmol, dissolved in 20 mL of absolute dichloromethane) were added dropwise. The cooling bath was removed, and the reaction was stirred for further 24 h at ambient temperature. Deionized H_2O of 200 mL was added, after phase separation the organic phase was extracted with diluted hydrochloric acid (1.5%), then with water and finally with aqueous Na_2CO_3 (10 wt.%) and subsequently dried over Na_2SO_4. The solvent was removed in vacuo. The residual crude product was purified by column chromatography (silica gel, cyclohexane/ethyl acetate (30:1)). Yield of compound **3**: 11.08 g (72% yield) of a white solid product.

Melting point: 109–110 °C. ^1H NMR (δ, 20 °C, $CDCl_3$, 500 MHz): 7.41, 7.39 (m, 4H, $ph^{3,5}$), 7.26 (m, 2H, ph^4), 7.13, 7.07 (d, 4H, $ph^{2,6}$), 6.45, 6.30 (m, 2H, $nb^{5,6}$), 3.79 (m, 1H, nb), 3.54 (s, 1H, nb), 3.42 (s, 1H, nb), 3.10 (m, 1H, nb), 1.80, 1.64 (d, 2H, nb). $^{13}C\{^1H\}$ NMR (δ, 20 °C, $CDCl_3$, 125 MHz): 173.1, 171.8 (2C, COOPh), 150.9 (2C, ph^1), 138.1, 135.3 (2C, $nb^{5,6}$), 129.6 (4C, $ph^{3,5}$), 126.1 (2C, ph^4), 121.6 (4C, $ph^{2,6}$), 48.3 (2C, $nb^{1,4}$), 47.6 (2C, $nb^{2,3}$), 46.2 (1C, nb^7). FTIR (thin

film on CaF_2, cm^{-1}): 3057 (w, aromatic C–H), 3098–2875 (w, aliphatic C–H), 1750 (s, C=O), 1592 (m, aromatic C=C), 1492 (w), 1456 (w), 1305 (w), 1263 (w), 1242 (w), 1192 (s, C–O–C ester), 1163 (s), 1150 (s), 1107 (w).

2.2.5. Poly(endo,exo-bicyclo[2.2.1]hept-5-ene-2,3-dicarboxylic acid, diphenyl ester) (poly-**3**)

To a solution of 5 g (14.98 mmol) of compound **3** in 45 mL of dichloromethane, 24.65 mg (29.91 μmol) of [$RuCl_2$-(PCy_3)(CHPh)] (Cy = cyclohexyl) dissolved in 10 mL of dry dichloromethane was added. The reaction mixture was stirred at room temperature for 24 h and then the reaction was stopped by adding 0.5 mL of ethylvinylether and the polymer was precipitated by dropping the solution into an excess of cold methanol. The precipitate was dried in vacuo. Yield: 5.01 g (99%) of a white solid. $M_n = 140{,}000\ g\ mol^{-1}$; $M_w = 159{,}000\ g\ mol^{-1}$; PDI = 1.1 (determined by SEC); T_g: 96.5 °C. ^1H NMR (δ, 20 °C, $CDCl_3$, 500 MHz): 7.20–7.70 (m, 10H ph), 5.73 (m, 2H, C=C nb), 3.64–2.93 (m, 4H, $nb^{1,2,3,5}$), 2.12–1.55 (m, 2H, nb^4). Elemental analysis: found C: 75.19, H: 5.51, O: 19.30%; calculated C: 75.43%, H: 5.43%, O: 19.14%. FTIR (thin film on CaF_2, cm^{-1}): 3028 (w, aromatic CH), 3004–2847 (m, aliphatic CH), 1767 (s, C=O), 1600 (w, aromatic C=C), 1509 (m, aromatic C=C), 1441 (w), 1373 (m), 1223 (s), 1197 (s), 1020 (m), 907 (m, C=C–H).

2.3. Characterization techniques

FTIR spectra were recorded with a Perkin–Elmer Spectrum One instrument (spectral range between 4000 cm^{-1} and 450 cm^{-1}). All FTIR spectra of the samples were taken in transmission mode. UV/vis spectra were measured with a Jasco V-530 UV/VIS spectrophotometer. All UV/vis spectra were taken in the absorbance mode. For spectroscopic measurements, polymer films were prepared on CaF_2 plates by spin casting from chloroform solutions. Weight and number average molecular weights (M_w and M_n) as well as the polydispersity index $PDI = M_w M_n^{-1}$ were determined by size exclusion chromatography (SEC) with the following setup: Merck Hitachi L6000 pump, separation columns from Polymer Standards Service (8 mm × 300 mm, STV 5 μm grade size; 10^6, 10^4, and 10^3 Å pore size), refractive index detector (model Optilab DSP Interferometric Refractometer) from Wyatt Technology. Polystyrene standards from Polymer Standard Service were used for calibration. All SEC runs were performed with chloroform as eluent. ^1H and ^{13}C NMR spectra were taken with a Varian INOVA 500 MHz spectrometer operating at 499.803 MHz and 125.687 MHz, respectively. Solvent residual peaks were used for referencing the NMR spectra to the corresponding values given in literature [21]. Differential scanning calorimetric (DSC) measurements were carried out with a Perkin–Elmer instrument (model Pyris Diamond) under a nitrogen flow of 20 mL min^{-1}. Glass transition temperatures (T_g) were read as the midpoint of change in heat capacity. Elemental analysis was carried out by the Microanalytical Laboratory of the University of Vienna (J. Theiner).

2.4. Determination of absorbance coefficients

To obtain the absorbance coefficients A in the infrared region, a liquid cell equipped with KBr windows was employed. The optical path length was 117 μm as determined with a precision gauge. Acetonitrile solutions of phenyl acetate, 2-hydroxyacetophenone and 4-hydroxyacetophenone were prepared with concentrations in the range 1.0–10.0 mmol L^{-1}. Quantitative FTIR measurements (in absorbance mode) showed that a linear relationship exists between the concentration of the compound and the absorbance at the wavenumber of the carbonyl group (phenyl acetate: ester band at 1750 cm^{-1}; 2-hydroxyacetophenone: ketone band at 1641 cm^{-1}; 4-hydroxyacetophenone: ketone band at 1675 cm^{-1}). In each case, the band height was determined by a tangent fit method. From linear regression the absorbance coefficients were calculated. Phenyl acetate: $A_{1750} = 420\ L\ mol^{-1}\ cm^{-1}$; 2-hydroxyacetophenone: $A_{1641} = 345\ L\ mol^{-1}\ cm^{-1}$; 4-hydroxyacetophenone: $A_{1675} = 320\ L\ mol^{-1}\ cm^{-1}$.

2.5. UV irradiation procedure

The unfiltered light of a polychromatic medium pressure mercury lamp (Heraeus) was used. All UV irradiations of polymer samples were conducted under inert gas atmosphere (nitrogen with a purity >99.95%). For these experiments, the light intensity (power density) at the sample surface was measured with a spectroradiometer (Solatell, Sola Scope 2000TM, measuring range from 230 to 470 nm). The integrated power density for the spectral range 230–400 nm was 45 mW cm^{-2}. For sample preparation, solutions of the corresponding polymers (10 g L^{-1} in chloroform) were spin-cast onto CaF_2 disks. The polymer samples were exposed for periods between 240 and 840 s. UV/vis and FTIR spectra were taken prior to and after UV illumination in order to monitor the progress of the photoreaction.

2.6. Ellipsometric measurements

For sample preparation, solutions of the corresponding polymers (10 g L^{-1} in chloroform) were spin-cast onto silicon wafers. Ellipsometric measurements were performed with a Woollam VASE spectroscopic ellipsometer (xenon short arc lamp, wavelength range 240–1100 nm, spectral bandwidth 4 nm). The implemented software uses the Levenberg–Marquardt fit algorithm. From ellipsometric data both the film thickness and the dispersion of the refractive index (Cauchy fit) were obtained.

2.7. Contact angle measurements

The surface tension γ of the sample surfaces was determined by measuring the contact angle with a Drop Shape Analysis System DSA100 (Krüss GmbH, Hamburg, Germany) using water and diiodomethane as test liquids (drop volume ~ 20 μL). The contact angles were obtained by means of the sessile drop method and they were measured within 2 s.

The mean values of five individual measurements were used, the reproducibility was within 2°. Based on the Owens–Wendt method, the surface tension γ as well as the dispersive and polar components (γ^D and γ^P) were evaluated [22].

3. Results and discussion

3.1. Syntheses

The photosensitive polymer poly(4-acetoxystyrene) (poly-**1**) was synthesized by free radical polymerization of commercial 4-acetoxystyrene (**1**) as depicted in Scheme 2. In contrast to this, monomers **2** and **3** were polymerized by catalytic ring-opening metathesis polymerization (ROMP). The synthetic routes to monomers **2** and **3** as well as their polymers poly-**2** and poly-**3** are outlined in Scheme 3. Starting from acryloyl chloride and cyclopentadiene, bicyclo[2.2.1]hept-5-ene-2-carboxylic acid chloride is obtained from a Diels–Alder reaction. Esterification with phenol then leads to monomer **2**. Poly(bicyclo[2.2.1]hept-5-ene-2-carboxylic acid, phenyl ester) (poly-**2**) was prepared in high yield using the ruthenium-based ''Grubbs catalyst''. For monomer **3**, fumaryl chloride was used instead of acryloyl chloride in the Diels–Alder reaction. Poly(*endo,exo*-bicyclo[2.2.1]hept-5-ene-2,3-dicarboxylic acid, diphenyl ester) (poly-**3**) was synthesized in an analogous manner. Both ROM polymerizations proceeded in high yields.

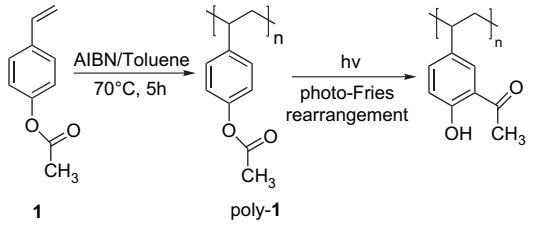

Scheme 2. Synthesis of poly(4-acetoxystyrene) (poly-**1**) and its photo-Fries rearrangement.

While the molar mass distribution of poly-**3** is low (polydispersity index, PDI = 1.1) as expected for ROM polymerizations, for poly-**2** a rather broad distribution of the molar mass was found (PDI = 1.9). One explanation for this finding may be some (unwanted) crosslinking in this polymer during synthesis and work-up. The glass transition temperatures (T_g) of poly-**2** and poly-**3** are well above room temperature (poly-**2**: 72 °C and poly-**3**: 96 °C). All polymers show excellent film forming properties when spin-cast from $CHCl_3$ solutions. Fully transparent and colourless films with optical quality were obtained from all three polymers.

3.2. UV/vis spectroscopy

The polymers under investigation absorb UV light up to a wavelength $\lambda \sim 280$ nm (peak maximum at $\lambda \sim 260$ nm). UV absorption in this range is typical of the phenyl chromophore with its $\pi-\pi^*$ transitions. The ester C=O group itself absorbs at around 190 nm ($\pi-\pi^*$) and with extremely low absorbance near 270 nm ($n-\pi^*$), while the C=C double bonds – present in poly-**2** and poly-**3** – absorb near 200 nm ($\pi-\pi^*$ transition). As an example, Fig. 1 displays the UV/vis spectra of a film of poly-**1** prior to and after flood UV illumination under nitrogen atmosphere with an energy density $E = 27$ J cm^{-2}. It can be seen that UV irradiation leads to a significant increase in UV absorption. For the irradiated sample of poly-**1**, two weak absorbance maxima localized at $\lambda =$ 260 nm and $\lambda = 330$ nm are observed. These changes indicate the formation of aromatic hydroxyketone units. For comparison, 4-hydroxyacetophenone displays UV absorbance maxima at $\lambda = 252$ nm and $\lambda = 326$ nm [23]. These absorptions are assigned to the $\pi-\pi^*$ and $n-\pi^*$ orbital transitions, respectively.

Similar results were obtained with the poly(norbornene esters) as shown in Figs. 2 and 3. Poly-**2** and poly-**3** exhibit spectral changes similar to those obtained for poly-**1**. An

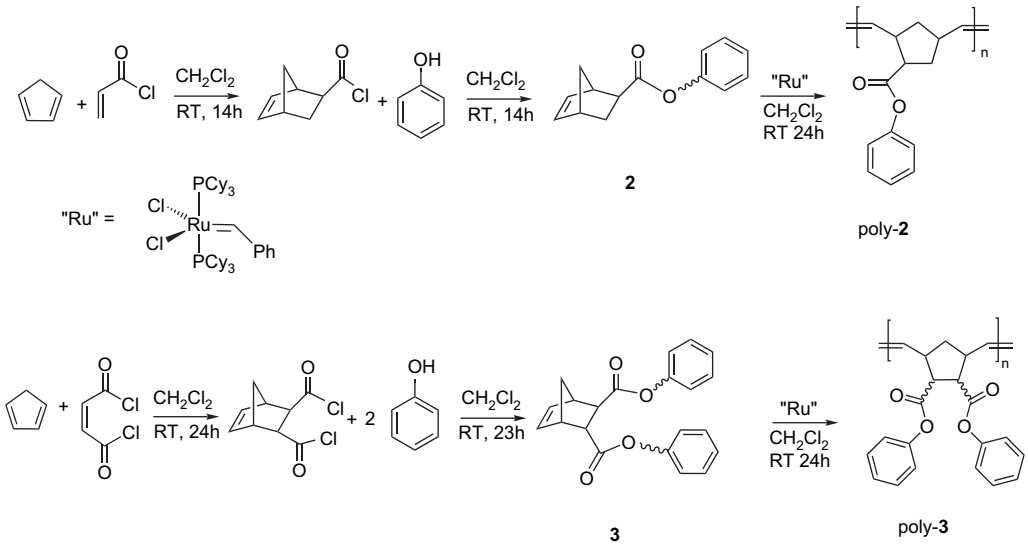

Scheme 3. Synthesis of monomers **2** and **3** and ring-opening metathesis polymerization (ROMP) to give poly-**2** and poly-**3**.

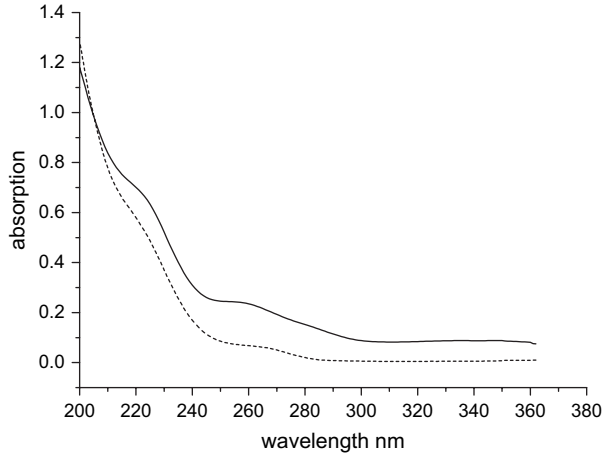

Fig. 1. UV spectra of a film of poly-**1** on KBr. Dotted line: prior to irradiation; solid line: after UV irradiation with an energy density $E = 27\ \mathrm{J\,cm^{-2}}$ ($\lambda = 230$–400 nm).

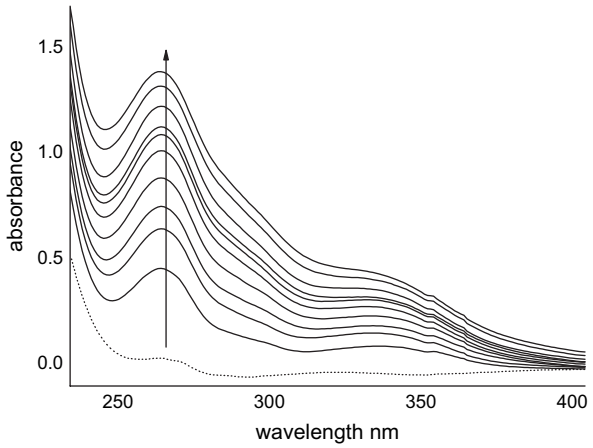

Fig. 3. UV spectra of a film of poly-**3** on KBr prior to (dotted line) and after prolonged UV irradiation (solid lines). Spectra were taken after irradiation with energy densities $E = 2.7$, 5.4, 8.1, 13.5, 18.9, 24.3, 29.7, 40.5, 67.5, 94.5 $\mathrm{J\,cm^{-2}}$ ($\lambda = 230$–400 nm).

evolution of absorption maxima at $\lambda = 260$ nm and $\lambda = 330$ nm is observed. Fig. 3 displays stacked UV spectra of poly-**3** which were recorded at intervals during prolonged UV illumination (up to 35 min) under nitrogen atmosphere. These spectra indicate that UV spectroscopy is a useful tool for following the kinetics of the photo-Fries rearrangement. However, it must be considered that aromatic–aliphatic ketones, which are produced as the acyl rearrangement product in the photo-Fries reaction, are photoreactive themselves. Indeed, photocleavage and hydrogen abstraction reactions as well as free radical reactions involving the C=C groups of the polynorbornene backbone may take place in poly-**2** and poly-**3** at later stages of the UV irradiation. For this reason a kinetic assay was performed with FTIR spectroscopy (vide infra).

3.3. FTIR spectroscopy

Since UV spectroscopy provides only limited information on the photoproducts of the polymers, FTIR spectra of the polymers were recorded prior to and after UV illumination. Moreover, the kinetics of the photo-Fries reaction was followed by quantitative FTIR spectroscopy.

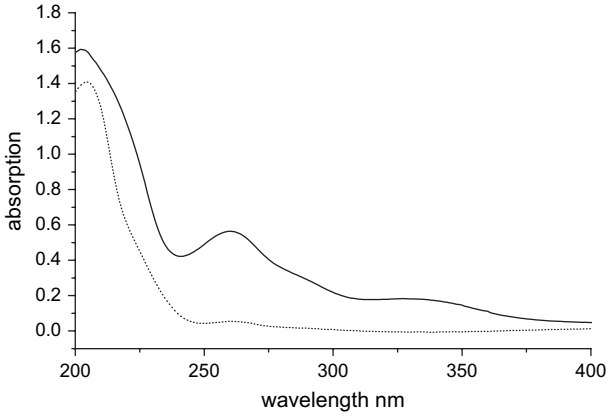

Fig. 2. UV spectra of a film of poly-**2** on KBr. Dotted line: prior to irradiation; solid line: after UV irradiation with an energy density $E = 21.6\ \mathrm{J\,cm^{-2}}$ ($\lambda = 230$–400 nm).

Fig. 4 shows detail FTIR spectra of a transparent film of poly-**1** after polychromatic irradiation with an energy density $E = 27\ \mathrm{J\,cm^{-2}}$ (measured in the range $\lambda = 230$–400 nm). In the spectrum of the non-irradiated film the signals at 1767 $\mathrm{cm^{-1}}$ (C=O stretch) and at 1197 $\mathrm{cm^{-1}}$ (asym. C–O–C stretch) are typical of the ester units. The position of these two bands exactly meets the expectation for esters R_1–(C=O)–O–R_2 with R_1 being an aliphatic unit and R_2 being a phenyl ring [24]. Other bands in this FTIR spectrum are typical of aliphatic groups (1373 $\mathrm{cm^{-1}}$: C–H deformation in the CH_3 units of the acetate group) and aromatic groups (1604 $\mathrm{cm^{-1}}$ and 1509 $\mathrm{cm^{-1}}$: aromatic ring vibration; 847 $\mathrm{cm^{-1}}$: C–H deformation in 1,4-disubstituted benzenes). The signal at 1013 $\mathrm{cm^{-1}}$ is related to the acetate group.

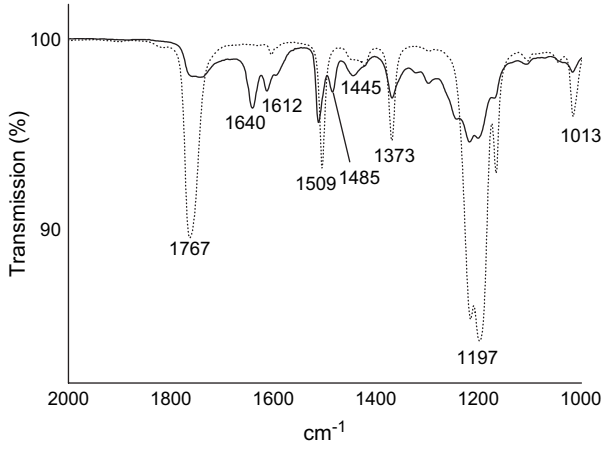

Fig. 4. FTIR spectra of a film of poly-**1** (film thickness approx. 0.5 μm) prior to (dotted line) and after irradiation (solid line) with an energy $E = 27\ \mathrm{J\,cm^{-2}}$ ($\lambda = 230$–400 nm). The depletion of the ester group (bands at 1767 $\mathrm{cm^{-1}}$ and 1197 $\mathrm{cm^{-1}}$) is accompanied by the evolution of the ketone (band at 1640 $\mathrm{cm^{-1}}$).

After UV irradiation, significant changes are observed in the FTIR spectrum of poly(4-acetoxystyrene) (poly-**1**). The signals of the phenyl ester group at 1767 cm^{-1} and 1197 cm^{-1} have almost quantitatively disappeared, also the signal at 1013 cm^{-1}. New bands are observable at 3400 cm^{-1} (not shown in the detail spectrum in Fig. 4), 1640 cm^{-1} and 1612 cm^{-1}. These signals indicate the formation of a hydroxyketone which is the expected photo-Fries product (cf. Scheme 2). The broad band at 3400 cm^{-1} stems from the O–H stretching vibration of hydroxyl groups, while the split carbonyl band with peak maxima at 1640 cm^{-1} and 1612 cm^{-1} is typical of aromatic–aliphatic ketones. For comparison, the FTIR spectrum of 2-hydroxyacetophenone, a low-molecular weight reference compound was recorded. For this compound a split carbonyl band at 1643 cm^{-1} and 1603 cm^{-1} is found. These FTIR data prove that in poly-(4-acetoxystyrene) the photo-Fries reaction proceeds as expected.

The FTIR spectra of poly-**2** and poly-**3** present a similar situation. Fig. 5 displays FTIR spectra of a film of poly-**2** (thickness approx. 6 μm) prior to and after irradiation with an energy density $E = 27\ J\ cm^{-2}$ (measured in the range $\lambda = 230–400$ nm). The depletion of the ester group (bands at 1745 cm^{-1}, 1193 cm^{-1}, and 1130 cm^{-1}) is accompanied by the evolution of a band at 1632 cm^{-1} which is assigned to the *ortho*-hydroxyketone. In addition to this, a weak signal appears at 1670 cm^{-1}. Considering the position of the C=O band in 4-hydroxyacetophenone (1675 cm^{-1}), this signal indicates the formation of *para*-hydroxyketone groups. The overall photoreaction in poly-**2** is depicted in Scheme 4. For poly-**3** essentially the same observations were made: the ester band at 1752 cm^{-1} depletes, and new carbonyl signals at 1632 cm^{-1} (*ortho*-hydroxyketone) and at 1670 cm^{-1} (*para*-hydroxyketone) are observed. FTIR spectra of poly-**3** are given in the supplementary data.

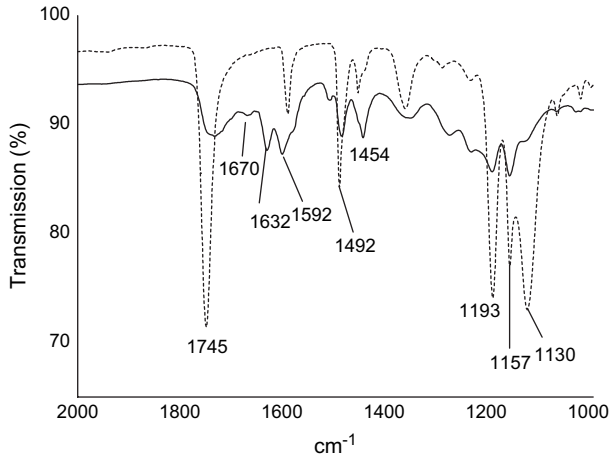

Fig. 5. FTIR spectra of a film of poly-**2** (film thickness approx. 6 μm) prior to (dotted line) and after irradiation (solid line) with an energy $E = 27\ J\ cm^{-2}$ ($\lambda = 230–400$ nm). The depletion of the ester group (bands at 1745 cm^{-1}, 1193 cm^{-1}, and 1130 cm^{-1}) is accompanied by the evolution of the ketones (band at 1632 cm^{-1} for the *ortho*-product and band at 1670 cm^{-1} for the *para*-product).

It is well known that the photo-Fries reaction also gives side products (e.g. decarboxylation products and free phenols). To estimate the photochemical yield of *ortho*- and *para*-hydroxyketone units (i.e. the photo-Fries products) in our polymers, the IR absorbance coefficients of model compounds were determined (acetoxybenzene: $A_{1750} = 420\ L\ mol^{-1}\ cm^{-1}$, 2-hydroxyacetophenone: $A_{1641} = 345\ L\ mol^{-1}\ cm^{-1}$ and 4-hydroxyacetophenone: $A_{1675} = 320\ L\ mol^{-1}\ cm^{-1}$). These absorbance coefficients were used for the estimation of the yield of the photo-Fries products. A comparison of the intensity of the ester carbonyl peak (1763 cm^{-1}) in non-irradiated poly-**1** and the *ortho*-hydroxyketone carbonyl peak (1641 cm^{-1}) showed that the yield of ketone in poly-**1** is between 30% and 35% after 10 min of irradiation ($E = 27\ J\ cm^{-2}$). This is the maximum value for this polymer: when the UV irradiation was prolonged, the intensity of the ketone peak decreased again. This finding is in good agreement with the data reported by Wilson [19]. For the new polymers, poly-**2** and poly-**3**, kinetic studies of the photo-Fries reaction were carried out by FTIR spectroscopy. Films of poly-**2** and poly-**3** were illuminated for defined periods, and absorbance FTIR spectra were recorded. The depletion of the ester signal and the evolution of the ketone bands were quantified by a tangent fit method using the absorbance coefficients A of the reference compounds (vide supra). The data are presented in Table 1 and in Figs. 6 and 7.

Fig. 6 refers to poly-**2**. The disappearance of the ester group follows a first order kinetics. The yield of the *ortho*-hydroxyketone passes through a maximum after 6 min of UV irradiation (corresponding to an energy density $E = 16.2\ J\ cm^{-2}$). At this point the conversion of the ester is approx. 57%, and the yield of the *ortho*-product is approx. 16%. As a minor reaction product, *para*-hydroxyketone units

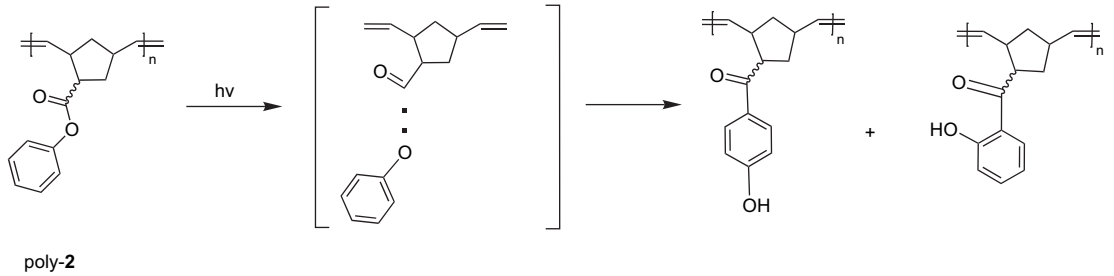

poly-**2**

Scheme 4. Photo-Fries rearrangement in poly-**2**.

Table 1
Reaction yields of *ortho*- and *para*-hydroxyketone units in poly-**1**, poly-**2**, and poly-**3** after UV irradiation

Polymer (min)	Irradiation time[a] (%)	Ester[b] (%)	*ortho*-Hydroxyketone[b] (%)	*para*-Hydroxyketone[b] (%)
Poly-**1**	0	100	0	–
	8	17	32	–
Poly-**2**	0	100	0	0
	6	43.3	16.4	3.3
Poly-**3**	0	100	0	0
	11	20.2	20.9	3.6

[a] Time for maximum yield of *ortho*-hydroxyketone obtained at a power density $P = 45$ mW cm^{-2}.
[b] For the characteristic FTIR signals used in this assessment, see text.

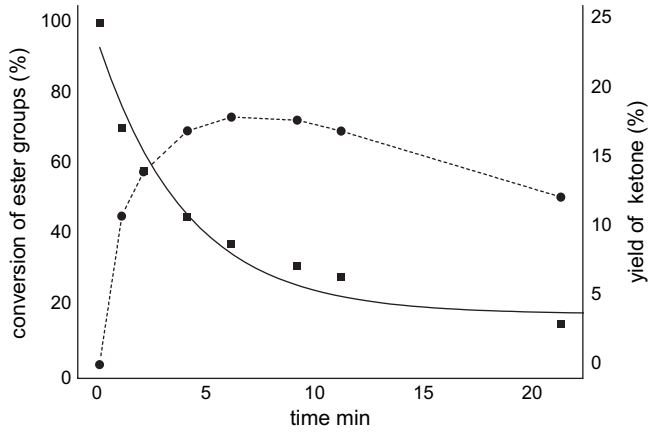

Fig. 6. Monitoring the photo-Fries rearrangement in poly-**2** by FTIR spectroscopy: depletion of the ester band at 1745 cm^{-1} and evolution of the *ortho*-hydroxyketone at 1632 cm^{-1}. UV irradiation was carried out at a power density of 45 mW cm^{-2} ($\lambda = 230$–400 nm).

are produced at a yield of approx. 3%. After prolonged irradiation the amount of ketone groups decreases again. This can be attributed to photoreactions of aromatic–aliphatic ketones, among them photocleavages and hydrogen abstraction reactions [25]. At the same time, the degradation of the ester groups continues, see Fig. 6. A very similar result is found for poly-**3**, see Fig. 7. Again the degradation of the ester proceeds with a first order kinetics. After 11 min of irradiation, the yield of *ortho*-hydroxyketone reaches its maximum with 21%. At this stage, 80% of the ester has reacted. Again, the yield of *para*-product is low (approx. 4%). From the exponential fit of the degradation of the ester units, similar half-life times τ are calculated (poly-**2**: $\tau = 4.0 \pm 0.8$ min; poly-**3**: $\tau = 3.6 \pm 0.6$ min). Summing up, the photochemical yield of hydroxyketones in polymeric media is comparably low (20–35%) whereas it can reach up to 90% for low-molecular compounds in dilute solutions [18].

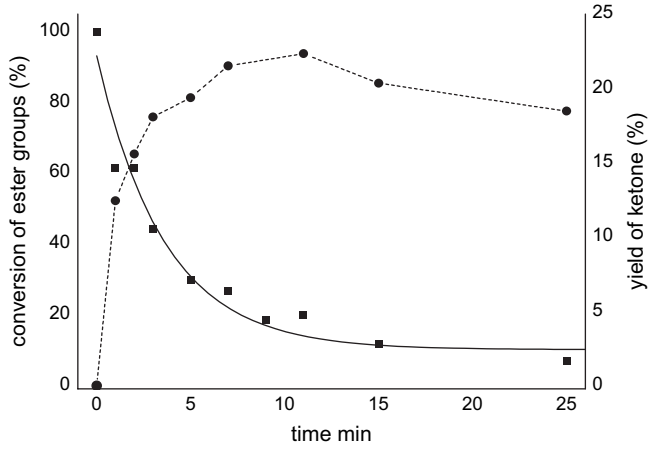

Fig. 7. Monitoring the photo-Fries rearrangement in poly-**3** by FTIR spectroscopy: depletion of the ester band at 1752 cm^{-1} and evolution of the *ortho*-hydroxyketone at 1634 cm^{-1}. UV irradiation was carried out at a power density of 45 mW cm^{-2} ($\lambda = 230$–400 nm).

3.4. Ellipsometry

The main focus of this research work was the preparation of polymers that undergo high refractive index changes upon UV irradiation. Such materials are desired for optical applications such as waveguiding, laser structures and holographic recording. Therefore the refractive index changes in the materials poly-**1**, poly-**2**, and poly-**3** were investigated by means of spectroscopic ellipsometry. Figs. 8–10 display the Cauchy fits of the dispersion of the refractive index both for pristine and UV illuminated films of the polymers under investigation. For these experiments, UV irradiation times were adjusted to obtain a maximum yield of ketone formation (cf. Figs. 6 and 7). In all polymers, a significant change in refractive index is observed upon UV irradiation as predicted for the acyl migration. For poly-**1** the refractive index increased from $n_{450} = 1.568$ (non-irradiated sample) to $n_{450} = 1.615$ after irradiation with a energy density $E = 27$ J cm^{-2}. The difference in the refractive index ($\Delta n = 0.047$) is remarkably high. In the case of poly-**2** the refractive index increased from $n_{450} = 1.594$ (non-irradiated sample) to $n_{450} = 1.636$ after irradiation with an energy density $E = 21.6$ J cm^{-2} and in the case poly-**3** from $n_{450} = 1.591$ (non-irradiated sample) to

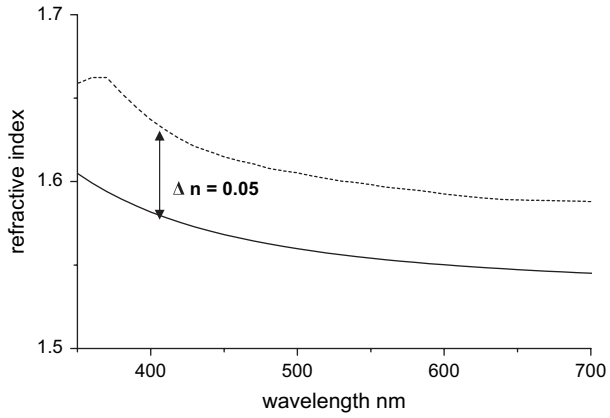

Fig. 8. Refractive index n of a film of poly-**1** on Si (film thickness approx. 150 nm) as a function of the wavelength λ (Cauchy fit). Solid line: prior to irradiation; dotted line: after irradiation with an energy $E = 27$ J cm^{-2} ($\lambda = 230$–400 nm).

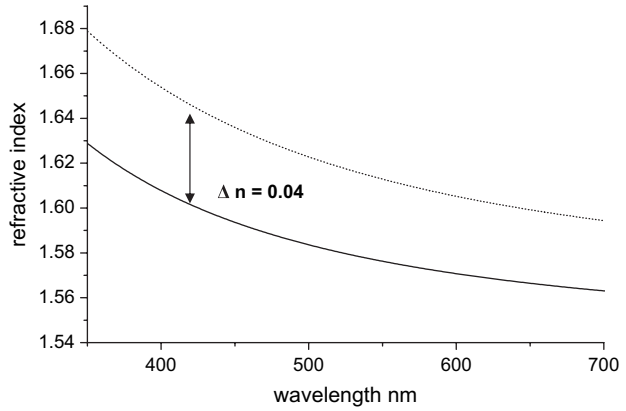

Fig. 9. Refractive index n of a film of poly-**2** on Si (film thickness approx. 85 nm) as a function of the wavelength λ (Cauchy fit). Solid line: prior to irradiation; dotted line: after irradiation with an energy $E = 21.6\ \mathrm{J\,cm^{-2}}$ ($\lambda = 230$–400 nm).

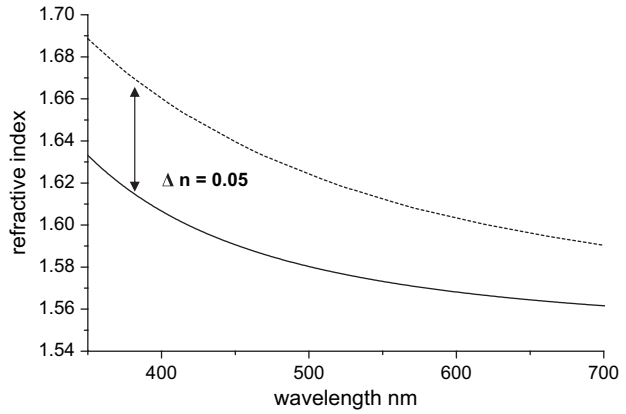

Fig. 10. Refractive index n of a film of poly-**3** on Si (film thickness approx. 70 nm) as a function of the wavelength λ (Cauchy fit). Solid line: prior to irradiation; dotted line: after irradiation with an energy $E = 21.6\ \mathrm{J\,cm^{-2}}$ ($\lambda = 230$–400 nm).

$n_{450} = 1.639$ after irradiation with an energy density $E = 21.6\ \mathrm{J\,cm^{-2}}$. These data correspond to a change of the refractive index of $\Delta n = 0.042$ and $\Delta n = 0.049$. Using shorter UV irradiation times, lower index changes are obtainable. It is instructive to compare these data to refractive index changes in other photoreactive polymers. Refractive index variations of more than $+0.003$ are commonly regarded as high [26,27]. For copolymers of vinyl cinnamate the photo-induced [2 + 2] cycloaddition results in a *decrease* of n by 0.02 [28], while in poly(4-vinylbenzyl thiocyanate) the SCN-NCS photoisomerization results in an *increase* of n by 0.03 [3]. Compared to these examples, the photo-Fries reaction yields very large refractive index changes in polymers.

3.5. Contact angle measurements

The photo-Fries rearrangement in poly-**1**, poly-**2** and poly-**3** generates phenolic OH groups at the polymer surface. To assess changes in surface polarity, contact angle measurements were carried out. Table 2 summarises the contact angles measured with water and diiodomethane as test liquids (sessile drop). The data on the surface tension γ and its dispersive (γ^D) and polar components (γ^P) — as calculated by the Owens–Wendt method — are also presented in Table 2. For all polymers, a slight decrease in the contact angle of water is observed after 8 min of UV illumination. At the same time, the contact angle of diiodomethane increases strongly. For example, for poly-**2** the contact angle of water drops from 83° to 81°, while the contact angle of diiodomethane increases from 30° to 50°. These data reflect a slightly increased hydrophilicity and a strongly increased oleophobicity as a result of the photo-Fries reaction.

Table 2
Contact angle and surface tension data for poly-**1**, poly-**2** and poly-**3** subjected to UV irradiation

Polymer	Irradiation time[a] (min)	θ (°) for H_2O[b]	θ (°) for CH_2I_2[b]	γ (mJ m^{-2})	γ^D (mJ m^{-2})	γ^P (mJ m^{-2})	Surface polarity (%)
Poly-**1**	0	97	22	47	47	0	0
	8	90	52	35	33	2	6.0
Poly-**2**	0	83	30	46	44	2	4.5
	8	81	50	38	34	4	11.8
Poly-**3**	0	89	34	44	43	1	2.3
	8	79	45	41	37	4	10.8

γ: surface tension; γ^D dispersive component, γ^P polar component; surface polarity $= 100(\gamma^P/\gamma)$.
[a] Power density $P = 45\ \mathrm{mW\,cm^{-2}}$.
[b] Contact angle (sessile drop).

A more quantitative picture is provided by the changes in surface tension and its components. In all cases, the overall surface tension γ drops as a result of UV illumination. This effect is mainly caused by a drop of the dispersive component γ^D which is only partly compensated by an increase of the polar component γ^P. For example, for poly-**2** the dispersive component γ^D of the surface tension decreases from $\gamma^D = 44\ \mathrm{mJ\,m^{-2}}$ to $\gamma^D = 34\ \mathrm{mJ\,m^{-2}}$, and at the same time the polar component γ^P increases from $\gamma^P = 2\ \mathrm{mJ\,m^{-2}}$ to $\gamma^P = 4\ \mathrm{mJ\,m^{-2}}$. As a result, the surface polarity ($(\gamma^P/\gamma)100$) of poly-**2** increases from approx. 4.5% to 11.8% although the overall surface tension γ decreases. Similar changes are observed for poly-**1** and poly-**3**, see Table 2. These results demonstrate that the photoreactions of aryl esters lead to significant changes in the surface properties of polymeric materials.

It is important to note that the photogenerated OH groups provide a possibility for a further surface modification by post-exposure reactions. This is the topic of ongoing research.

4. Conclusion

In this contribution, we have explored the photo-Fries reaction in polymers with the aim to achieve high refractive index changes upon UV irradiation. Starting with an investigation of the known polymer poly(4-acetoxystyrene), we have successfully transferred the concept of photo-induced acyl shifts to derivatives of poly(norbornene) obtained by ring-opening metathesis polymerization (ROMP). The progress of the

photo-Fries rearrangement can be followed both by UV and FTIR spectroscopies. In contrast to low-molecular weight compounds, the maximum yield of hydroxyketone groups in the investigated polymers only amounts to 20–35%. Yet these photoreactive polymers exhibit large refractive index changes Δn up to +0.05. This value is more than sufficient for many optical applications such as waveguiding and index gratings. Moreover, the photo-Fries rearrangement leads to significant changes in the surface properties of the polymers by the generation of phenolic OH groups. Due to the fact that polymers bearing aryl esters are easily accessible the photo-Fries rearrangement can be utilized in a variety of functional polymeric materials.

Acknowledgments

The authors wish to thank *J. Hobisch* for carrying out the SEC analysis, *P. Kaschnitz* for NMR measurements and *S. Temmel* for assistance during contact angle measurements and for helpful discussions. Financial support by *FWF* (Fonds zur Förderung der Wissenschaftlichen Forschung, Vienna) is gratefully acknowledged. This work was initiated within the framework of the *Austrian Nanoinitiative* (RPC 0700 – RP 0703) and subsequently continued within the *NFN Research Network* (funded by *FWF*, project no. S9702-N08 ''Design and application of tunable surfaces based upon photoreactive molecules'').

Appendix A. Supplementary data

Supplementary data associated with this article can be found in the online version, at doi:10.1016/j.polymer.2007.01.041.

References

[1] Lessard RA, Chankakoti R, Gurusamy M. Holographic recording materials. In: Krongauz VV, Trifunac AD, editors. Processes in photoreactive polymers. New York: Chapman and Hall; 1995. p. 305–67.
[2] Coufal HJ, Psaltis D, Sincerbox GT, editors. Holographic data storage. Berlin: Springer; 2000.
[3] Langer G, Kavc T, Kern W, Kranzelbinder G, Toussaere E. Macromol Chem Phys 2001;202:3459–67.
[4] Kavc T, Kern W, Zenz C, Leising G, Kranzelbinder G, Toussare E. Monatsh Chem 2001;132:531–40.
[5] Lex A, Trimmel G, Kern W, Stelzer F. J Mol Catal A 2006;254:174–9.
[6] Slugovc C. Macromol Rapid Commun 2004;25:1283–97.
[7] Grubbs RH, editor. Handbook of metathesis. Weinheim: Wiley VCH; 2003.
[8] Bellus D. Adv Photochem 1971;8:109.
[9] Anderson JC, Reese CB. Proc Chem Soc 1960;217.
[10] Weast RC, editor. CRC handbook of chemistry and physics. 62nd ed. Boca Raton, Florida: CRC Press, Inc.; 1981–1982.
[11] Gillberg-LaForce GE, Yokley E, Kuder JE, Fernekess E. US Patent 5,128,223, Hoechst Celanese Corp; 1992.
[12] Kalmus CE, Hercules DM. J Am Chem Soc 1974;96(2):449–56.
[13] Miranda MA, Galindo F. Photo-Fries reaction and related processes. In: Horspool WM, editor. CRC handbook of organic photochemistry and photobiology. 2nd ed. Boca Raton: CRC Press; 2004 [chapter 42].
[14] Lochbrunner S, Zissler M, Piel J, Riedle E, Spiegel A, Bach T. J Chem Phys 2004;120(24):11634–9.
[15] Kopezky J. Photochemistry: a visual approach. New York: VCH; 1992 [chapter 10].
[16] Finnegan RA, Knutson D. Tetrahedron Lett 1968;9(30):3429–32.
[17] Weiqiang G, Abdallah DJ, Weiss RG. J Photochem Photobiol A Chem 2001;139:79–87.
[18] Bellus D, Hrdlovic P. Chem Rev 1967;67(6):599–609.
[19] Fréchet JMJ, Tessier TG, Wilson CG, Ito H. Macromolecules 1985;18:317–21.
[20] Ishihara K, Kurihara H, Matsumoto M, Yamamoto H. J Am Chem Soc 1998;120(28):6920–30.
[21] Gottlieb HE, Kotylar V, Nudelman A. J Org Chem 1997;62(12):7512–5.
[22] Kaneko M, Sato H. Macromol Chem Phys 2004;205(2):173–8.
[23] UV ATLAS of organic compounds, vol. 2. Weinheim: Verlag Chemie; 1966.
[24] Socrates G. Infrared characteristic group frequencies. 2nd ed. Chichester: Wiley; 1994 [chapter 10].
[25] Crivello JV, Dietliker K. In: Bradley G, editor. Photoinitiators for free radical, cationic and anionic photopolymerisation, vol. 3. Chichester: J Wiley & Sons; 1998.
[26] Assaid I, Bosc D, Hardy I. J Phys Chem B 2004;108(9):2801–6.
[27] Biteau J, Chaput F, Lahlil K, Boilot JP, Tsivgoulis GM, Lehn JM, et al. Chem Mater 1998;10(7):1945–50.
[28] Nagata A, Sakaguchi T, Ichihashi T, Miya M, Ohta K. Macromol Rapid Commun 1997;18:191–6.